PERFORMANCE IMPROVEMENT OF MANIPULATOR ACTUATED BY PNEUMATIC ARTIFICIAL MUSCLES BASED ON SYNERGETIC CONTROL AND SOCIAL SPIDER OPTIMISATION ALGORITHM

ALAQ F. HASAN, HADEER A. RAHEEM*, RAJAA HUSSEIN

Middle Technical University, Technical Engineering Collage Baghdad, Mechatronics Engineering, 8998+QHJ, Baghdad, Iraq

* corresponding author: hadeerasaadtec@mtu.edu.iq

ABSTRACT. The manipulator actuated by pneumatic artificial muscles (PAM) is a widely used type of robotic arm in industrial automation. However, its performance can be limited by non-linear dynamics and uncertainties in the system. To overcome these limitations, this paper proposes a synergetic control strategy (SACT) to improve the performance of the SACT, a social spider optimisation algorithm (SSO) has been suggested for adjusting its parameters. To verify the performance of a PAM-actuated manipulator based on an optimal SACT controller, a computer simulation study was conducted using MATLAB software. Moreover, a comparison study between the optimal synergetic algorithm control theory and the optimal sliding mode controller (SMC) has been made in terms of robustness and transient behaviour characteristics. The provided simulation results have shown that the SACT controller exhibited quicker convergence towards the desired trajectory and maintained a lower steady-state error as compared to the SMC controller. Additionally, the SACT controller demonstrated more resilience to variations in parameters and showed more robust characteristics.

KEYWORDS: PAM-actuated manipulator, synergetic algorithm control theory, sliding mode controller, social spider optimisation algorithm.

1. INTRODUCTION

The actuator is an essential part of some systems that is responsible for transferring energy from one form to another, e.g. the mechanical motion interprets an explicit nature of any interaction between the parts of a system and its environment. A recent study in robotic systems technology suggests that the interface format, or mechanism movement, could be changed from geared motors to a softer biological idea of bone-tendon-muscle. This trend will ensure that machines and humans interact closely, as well as that there is safety, redundancy, self-repair, functional and physical softness. As a result, any modern actuation system must include the advantageous characteristics of traditional actuators, including correct design features, such as the ratio between the force and the actuator volume and extra operational life. The pneumatic actuators were one of these modern actuation technologies, such as cylinders, which are widely used in factory automation systems. Recently, robotics has begun to use pneumatics as the main power source of motion. One of the main advantages of pneumatic actuators is their low weight and their inherent accommodating behaviour as compared to hydraulic actuators [1–3].

One of the lesser known types of pneumatic actuator is the so-called pneumatic artificial muscle. These are the inverse form of the bellows, i.e. they have some similarities in the inflation process. Their force is dependent on pressure, in addition to their dependence on the state of inflation, and that creates a second source of spring-like behaviour. PAM's weight is extremely light because the element of their core is a membrane, thus, compared to cylinders, they can transfer the same amount of energy, as long as they are operating at the same ranges of pressure and volumes. For these reasons, PAMs have great potential and advantages to be used in bio-robotic systems with reliable performance [4].

Pneumatic muscle-based systems are characterised by high complexity, nonlinearity, and uncertainty in their parameters. Several researchers have suggested various control schemes to tackle the control challenges of pneumatic muscle-based systems. The following studies address the control techniques commonly used to control PAM-actuated systems:

- Al-Jodah and Khames [5] presented two control strategies to control the angular position of a single link robotic arm actuated by a pair of PAMs. The first one is sliding mode control based on a super-twisting algorithm and the other is a classic sliding mode control. The main objective of this work is to reduce the effect of the chattering problem that is commonly associated with SMC design. To solve this problem, the researcher used the super twisting-algorithm. The computer simulation has verified a low tracking error in terms of a sliding mode control based on the super-twisting algorithm as compared to classical sliding mode control. Moreover, a sliding mode control based on the super-

twisting algorithm shows a solid durability against uncertainty in system parameters.

- Scaff et al. [6] used a PID controller to control the angular position of a single link robotic arm actuated by McKibben PAMs and to improve the performance of the PID controller, they used Simulated Optimisation Algorithm (SOA). This study did not show the efficiency of the controlled system in the presence of variation in the parameters of the system.

- Boudoua et al. [7] presented a design of a super-twisting sliding mode controller based on neural network to control the angular position of a PAM robotic arm. To estimate the unknown dynamics of the robot, the study used a two-neural network layer with online adaptive learning law. The work is lacking in the capability to remove the chattering problem in the control signal.

- Repperger et al. [8] applied the gain-scheduled controller to control the angular position of a large-scale pneumatic muscle actuator. Through numerous experiments of transient and steady-state responses, the scheduled gains had been established. The study did not show the efficiency of the proposed controller in the presence of variations in the parameters of the system.

- Enzevaee et al. [9] proposed a fuzzy logic controller based on an Active Force Control technique to control the angular position of a manipulator with one degree of freedom. The obtained results of the proposed controller show the controller's ability to compensate for the subjected disturbances robustly.

- Farag and Azlan [10] applied the adaptive backstepping controller to control the angular position of Anthropomorphic Robot Hand at PAM actuators. The adaptive controller has been integrated with the PID controller to form a hybrid controller. The adaptive law has been obtained to estimate the uncertainty in the values of the system parameters. The simulation results have validated the tracking performance based on the proposed controller.

The synergetic control strategy theory is based on a state-space theory that focuses on the design and control of extremely complicated systems. This control strategy can allow the system's states to develop on the designer's selected invariant manifolds while achieving the intended performance in the presence of uncertainties and disruptions [11]. In view of this point, a brief discussion of a research relevant to the synergetic control strategy theory will be presented:

- Nechadi et al. [12] proposed a synergetic control strategy to satisfy the output voltage of the DC-DC Boost converter at the required level. The proposed controller shows high performance competence despite the nonlinear behaviour of the system.

- Al-Dujaili et al. [13] investigated an adaptive control design using adaptive synergetic control strategy
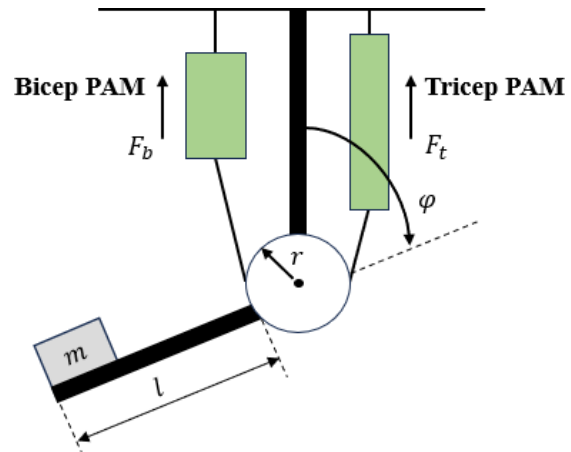
FIGURE 1. One degree of freedom manipulator actuated by PAMs.

theory to mitigate the effect of vibrations in a building structure due to earthquake action. The study involved a single-degree-of-freedom building, and numerical simulation demonstrated the ability of the proposed scheme to significantly reduce vibrations from the impact of the earthquake

- Al-Khazraji et al. [14] presented the design of synergetic control strategy theory to improve the position tracking accuracy of a ball and beam system. Compared to a classic state feedback controller, the synergetic control strategy theory exhibited better performance in terms of stability, robustness characteristics, and finite-time convergence of position error.

The major contributions addressed by this work can be summed up as:

- developing a SACT to control the angular position of a PAM-actuated single link robotic arm,

- optimal tuning of SACT parameters to improve the performance of an SACT-based PAM-actuated manipulator,

- carrying out a comparative study between SACT and SMC algorithms in terms of robustness and transient behaviour characteristics.

Subsequent sections of this paper are organised as follows: Section 2 presents the modelling of a PAM-actuated manipulator. Section 3 presents the design and stability analysis of SACT and SMC algorithms. In addition, this section presents the optimisation problem and its SSO-based solution. Section 4 presents a computer simulation to validate the performance of the proposed controllers. Finally, the conclusions reached based on the results of the numerical simulation has been highlighted in Section 5.

2. MATHEMATICAL MODEL

The mathematical model of a PAM-actuated single link robotic arm had been derived and performed previously in [5, 15]. Figure 1 illustrates the general

concept of the PAM-actuated single link robotic arm whereas its equation of motion is as follows:

$$(ml^2 + i)\ddot{\varphi} + mgl\cos\varphi = T, \tag{1}$$

where the mass at the end point of the robotic arm is denoted by symbol m, the length of the arm is represented by symbol l, the gravitational acceleration is denoted by symbol g, the rotation angle and angular acceleration of the arm are denoted by the symbols φ and $\ddot{\varphi}$, respectively, the moment of inertia for the robotic arm is denoted by symbol i, and lastly, T, which stands for the generated torque by the bicep and tricep PAMs and required to rotate the link. The torque equation is given as:

$$T = (F_t(.) - F_b(.))r, \tag{2}$$

Where, r is the radius of the pulley and $F_t(.)$, $F_b(.)$ are the tricep and bicep forces that are generated from PAMs, respectively. The mathematical model of PAMs [5], which have been used to find $F_t(.)$ and $F_b(.)$, had been derived as follows:

$$F_t(.) = -K_t(x_t)x_t - B_t(\dot{x}_t)\dot{x}_t + P_t, \tag{3}$$
$$F_b(.) = -K_b(x_b)x_b - B_b(\dot{x}_b)xb + Pb, \tag{4}$$

where (t,b) stand for the tricep and bicep PAMs, respectively. Hence, $K_t(x_t)$ and $K_b(x_b)$ are the nonlinear function coefficients of the spring of the tricep and bicep PAM positions, respectively. $B_t(\dot{x}_t)$ and $B_t(\dot{x}_t)$ are the nonlinear function coefficients of the damper of the tricep and bicep PAM velocities, respectively. x_t and x_b are the amount of contraction in the bicep and tricep PAMs, respectively. $\dot{x}_t$ and $\dot{x}_b$ are the velocities of tricep and bicep PAMs in the contraction case, respectively. P_t and P_b are the pressures for the two PAMs [4]. By taking into consideration $i = (t,b)$, then $K_i(x_i)$ and $B_i(\dot{x}_i)$ are given by:

$$K_i(x_i) = k_{1i}x_i^2 + k_{2i}x_i + k_{3i}, \tag{5}$$
$$B_i(\dot{x}_i) = b_{1i}\dot{x}_i^2 + b_{2i}\dot{x}_i + b_{3i}, \tag{6}$$

where k_{1i}, k_{2i}, k_{3i}, b_{1i}, b_{2i}, b_{3i} are constants. There are two states of work for these constants, the first is when the PAM is inflated, and the second is when the PAM is in the deflated state. The state of the bicep and tricep PAMs can be explained as follows:

$$\dot{\varphi} < 0 \text{ in case of } \begin{cases} \text{bicep inflacted,} \\ \text{tricep deflated,} \end{cases}$$
$$\dot{\varphi} > 0 \text{ in case of } \begin{cases} \text{bicep deflacted,} \\ \text{tricep inflated.} \end{cases} \tag{7}$$

Thus, the bicep and tricep PAM pressure equations can be written as:

$$P_t = P_{0t} + \Delta P, \tag{8}$$
$$P_b = P_{0b} + \Delta P, \tag{9}$$

where P_{0t} and P_{0b} are considered to be the initial pressures. ΔP is the difference between the two pressures of the tricep and bicep which would be the system's control input. Now, x_t and x_b are the amounts of muscle contraction calculated as:

$$x_t = (\frac{\pi}{2} + \varphi)r, \qquad \dot{x}_t = r\dot{\varphi}, \tag{10}$$
$$x_b = (\frac{\pi}{2} - \varphi)r, \qquad \dot{x}_b = -r\dot{\varphi}, \tag{11}$$

where $\frac{\pi}{2}$ is presumed to be the null position at which the value of x_t and x_b is zero. Now, substitute Equations (8) and (9) in Equations (3) and (4), then substitute the resulting two equations in Equation (2), and the resulting equation is as follows:

$$T = (-K_t(x_t)x_t - B_t(\dot{x}_t)\dot{x}_t + P_{0t} + \Delta P \\ + K_b(x_b)x_b + B_b(\dot{x}_b)x_b - P_{0b} + \Delta P)r. \tag{12}$$

Then, make the substitution of both Equations (5) and (6) in Equation (12):

$$T = (-(k_{1t}x_t^2 + k_{2t}x_t + k_{3t})x_t \\ - (b_{1t}\dot{x}_t^2 + b_{2t}\dot{x}_t + b_{3t})\dot{x}_t + P_{0t} + \Delta P \\ + (k_{1b}x_b^2 + k_{2b}x_b + k_{3b})x_b \\ + (b_{1b}\dot{x}_b^2 + b_{2b}\dot{x}_b + b_{3b})\dot{x}_b - P_{0b} + \Delta P)r. \tag{13}$$

Finally, substitute Equations (10) and (11) in Equation (13), then substitute the resulting equation in Equation (1), and the resulting equation is as follows:

$$\left.\begin{aligned}
\ddot{\varphi} &= \delta_1\varphi^3 + \delta_2\varphi^2 + \delta_3\varphi + \delta_4\dot{\varphi}^3 \\
&\quad + \delta_5\dot{\varphi}^2 + \delta_6\dot{\varphi} + \delta_7\cos\varphi + \delta_8 + bu, \\
u &= \Delta P, \\
\delta_1 &= \frac{-r^3(k_{1b} + k_{1t})}{ml^2 + i}, \\
\delta_2 &= \frac{\frac{3\pi r^4}{2}(k_{1b} - k_{1t}) + r^3(k_{2b} - k_{2t})}{ml^2 + i}, \\
\delta_3 &= \frac{-\frac{3\pi r^4}{2}(k_{1b} - k_{1t})}{ml^2 + i} \\
&\quad + \frac{\pi r^3(k_{2b} + k_{2t}) + r^2(k_{3b} + k_{3t})}{ml^2 + i}, \\
\delta_4 &= \frac{-r^4(b_{1b} + b_{1t})}{ml^2 + i}, \\
\delta_5 &= \frac{r^3(b_{2b} - b_{2t})}{ml^2 + i}, \\
\delta_6 &= \frac{-r^2(b_{3b} - b_{3t})}{ml^2 + i}, \\
\delta_7 &= \frac{glm}{ml^2 + i}, \\
\delta_8 &= \frac{r(P_{0b} - P_{0t}) + \frac{\pi r^4}{8}(k_{1t} - k_{1b})}{ml^2 + i} \\
&\quad + \frac{\frac{\pi r^3}{4}(k_{2t} - k_{2b}) + \frac{\pi r^2}{2}(k_{3t} - k_{3b})}{ml^2 + i}, \\
b &= \frac{2r}{ml^2 + i}.
\end{aligned}\right\} \tag{14}$$

The system can be represented as follows, taking the uncertainty into consideration:

$$\left.\begin{aligned}
\ddot{\varphi} &= f_0 + \Delta f + bu, \\
f_0 &= \delta_1 \varphi^3 + \delta_2 \varphi^2 + \delta_3 \varphi + \delta_4 \dot{\varphi}^3 \\
&\quad + \delta_5 \dot{\varphi}^2 + \delta_6 \dot{\varphi} + \delta_7 \cos \varphi + \delta_8, \\
\Delta f &= \Delta \delta_1 \varphi^3 + \Delta \delta_2 \varphi^2 + \Delta \delta_3 \varphi + \Delta \delta_4 \dot{\varphi}^3 \\
&\quad + \Delta \delta_5 \dot{\varphi}^2 + \Delta \delta_6 \dot{\varphi} + \Delta \delta_7 \cos \varphi + \Delta \delta_8,
\end{aligned}\right\} \quad (15)$$

where δ_i is the nominal values and $\Delta \delta_i$ represent the uncertainty in the value of the system parameters.

3. CONTROL THEORY

Two control theories have been used in this work to control the system with a modern optimisation algorithm to obtain the optimal parameter for the controllers.

3.1. SLIDING MODE CONTROL (SMC) ALGORITHM

In sliding mode control, the control signal can typically be broken down into two parts. The first part is known as "the equivalent control", which represents both the sliding surface and the system dynamics. The other part is referred to as "the switching control", which maintains the system dynamics on the sliding surface [16, 17].

Firstly, the sliding surface could be defined as:

$$s = ce + \dot{e}, \quad (16)$$

where s and c are the sliding surface and the sliding coefficient, respectively, whereas e and $\dot{e}$ can be defined as the tracking error and the tracking error derivative, respectively. These two parameters are formulated as:

$$\begin{cases} e = \varphi - \varphi_r, \\ \dot{e} = \dot{\varphi} - \dot{\varphi}_r, \end{cases} \quad (17)$$

where φ and φ_r are the actual trajectory and the desired trajectory, respectively. The time derivative of Equation (16) is:

$$\begin{aligned} \dot{s} &= \ddot{e} + c\dot{e}, \\ \dot{s} &= \ddot{\varphi} - \ddot{\varphi}_r + c\dot{e}. \end{aligned} \quad (18)$$

As previously mentioned, the control law consists of two parts, equivalent and switching, thus:

$$u = \frac{1}{b} (u_{eq} + u_{sw}). \quad (19)$$

Equivalent control, u_{eq}, was proposed by Filipov as a means of controlling the system without taking external disturbances and uncertainties into account. By setting the sliding surface's derivative equation to zero, to keep the controlled variable on the surface, the equivalent component can be determined based on the equation:

$$u_{eq} = -f_o + \ddot{\varphi}_r - c\dot{e}. \quad (20)$$

In conventional SMCs, switching control u_{sw} is usually defined as:

$$u_{sw} = -k \operatorname{sign}(s), \quad (21)$$

where k and $k \operatorname{sign}(s)$ are the positive constant and symbolic function, respectively, that is defined by:

$$\operatorname{sign}(s) = \begin{cases} -1 & \text{if } s < 0, \\ 0 & \text{if } s = 0, \\ +1 & \text{if } s > 0. \end{cases} \quad (22)$$

We can perform the control law as:

$$u = \frac{1}{b}(-f_o + \ddot{\varphi}_r - c\dot{e} - k \operatorname{sign}(s)). \quad (23)$$

For emphasising the asymptotic stability of the PAM system via SMC, the Lyapunov function has been determined as:

$$V = \frac{1}{2}s^2. \quad (24)$$

Taking the first derivative of time for Equation (24), we get:

$$\begin{aligned} \dot{V} &= s\dot{s}, \\ \dot{V} &= s \left(f_o + \Delta f + bu - \ddot{q}_r + \gamma \dot{e}\right). \end{aligned} \quad (25)$$

Assumption 1: Parametric uncertainties in the system Δf are assumed to be unknown but bounded $|\Delta f| \leq f_{\max}$.

Now, substituting Equation (23) into Equation (25), we get:

$$\dot{V} = s \left(-k \operatorname{sign}(s) + \Delta f\right). \quad (26)$$

Remark 1: According to Equation (26), the stability of the PAM system based on SMC is ensured if k is chosen such that $k \geq f_{\max} \geq |\Delta f|$.

To mitigate the problem of chattering, which is a common issue in a conventional sliding mode control, an approximation signum function is used as a substitute for the sign function [18]:

$$\operatorname{sign}(s) \approx \frac{2}{\pi} \tanh(\beta s), \quad (27)$$

where β is a controller design parameter. Now, we can perform the control law as:

$$u = \frac{1}{b} \left(-f_o + \ddot{\varphi}_r - c\dot{e} - \frac{2k}{\pi} \tanh(\beta s)\right). \quad (28)$$

Figure 2 shows the control scheme of a PAM-actuated manipulator system based on the sliding mode controller.

3.2. SYNERGETIC CONTROL APPROACH

Kolesnikov [19] introduced the synergetic control approach, which involves starting the synergetic synthesis process by selecting a macro variable. This variable is a function of the system states:

$$\sigma = \sigma(x, t). \quad (29)$$
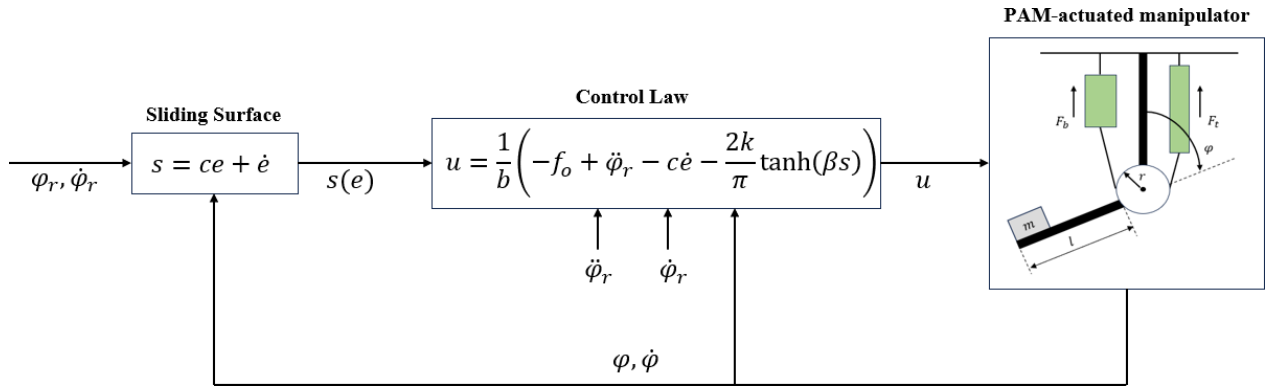
FIGURE 2. PAM-actuated manipulator controlled by SMC.

The macro-variable value is denoted by σ and this variable can be determined by a user-defined function, $\sigma(x, t)$, a function of time and system state variable. Thus, the designer of the control has the flexibility of selecting the characteristics of the macro-variable based on various factors, such as response time, control parameters, limitations of the command, etc. The main objective of the synergetic control approach is to push the system states to work on the $\sigma = 0$ manifold [12, 20, 21]. That helps the desired macro-variable dynamic evolution to be determined as:

$$\lambda \dot{\sigma} + \sigma = 0. \qquad (30)$$

When the macro-variable becomes equal to zero, design parameter λ determines the speed at which the closed-loop system converges to the manifold. But, $\dot{\sigma}$ defines the derivative of the aggregated macro-variable. Then, the solution of the differential equation is obtained as the following function:

$$\sigma(t) = \sigma_0 \, e^{-\frac{t}{\lambda}}. \qquad (31)$$

$\sigma(t)$ is attracted to $\sigma = 0$ from any initial condition σ_0. The chain rule of differentiation gives:

$$\dot{\sigma} = \frac{d\sigma}{dx} \frac{dx}{dt}. \qquad (32)$$

By combining Equations (30) and (32), we obtain:

$$\lambda \frac{d\sigma}{dx} f(x, u, t) + \sigma = 0. \qquad (33)$$

After solving Equation (33) for u, the controller law can be expressed as:

$$u = g(x, \sigma, \lambda, t). \qquad (34)$$

The equation demonstrates that the controller's characteristics can be selected by the designer through the choice of a particular control parameter λ and a proper macro-variable.

For controlling a PAM system by using a synergetic control algorithm, the following macro-variable has been considered:

$$\sigma = \dot{e} + \gamma e. \qquad (35)$$

Now, by using the substitution of Equation (35) into Equation (30), we obtain:

$$\lambda(\ddot{e} + \gamma \dot{e}) + \sigma = 0, \qquad (36)$$

then, by substituting Equation (15) into Equation (36) with rearranging, we obtain:

$$\lambda(\ddot{q} - \ddot{q}_r + \gamma \dot{e}) + \sigma = 0,$$
$$\lambda(f_o + \Delta f + bu - \ddot{q}_r + \gamma \dot{e}) + \sigma = 0.$$

Thus, the control action equation becomes:

$$u = \frac{1}{b}(-f_o + \ddot{q}_r - \gamma \dot{e}) - \frac{\sigma}{\lambda b}. \qquad (37)$$

For emphasising the asymptotic stability of the PAM system via SACT, the below Lyapunov function has been selected:

$$V = \frac{1}{2}\sigma^2. \qquad (38)$$

By taking the derivative of time for Equation (38), we get:

$$\dot{V} = \sigma \dot{\sigma},$$
$$\dot{V} = \sigma \left(f_o + \Delta f + bu - \ddot{q}_r + \gamma \dot{e} \right), \qquad (39)$$

and by substituting Equation (37) into Equation (39), we get:

$$\dot{V} = \sigma \left(-\frac{\sigma}{\lambda} + \Delta f \right). \qquad (40)$$

Note that for all $t \geq 0$, V is positive definite and $\dot{V}$ is negative definite if and only if $\frac{\sigma}{\lambda} \geq f_{\max} \geq |\Delta f|$. Figure 3 shows the control scheme of a PAM-actuated manipulator system based on the synergetic control approach.

3.3. PARAMETERS OPTIMISATION BASED ON SOCIAL SPIDER OPTIMISATION ALGORITHM

The SACT design parameters must be modified to provide the optimum controller performance for the PAM-actuated manipulator system. The trial-and-error approach of determining or modifying these parameters is inefficient and fails to produce optimal
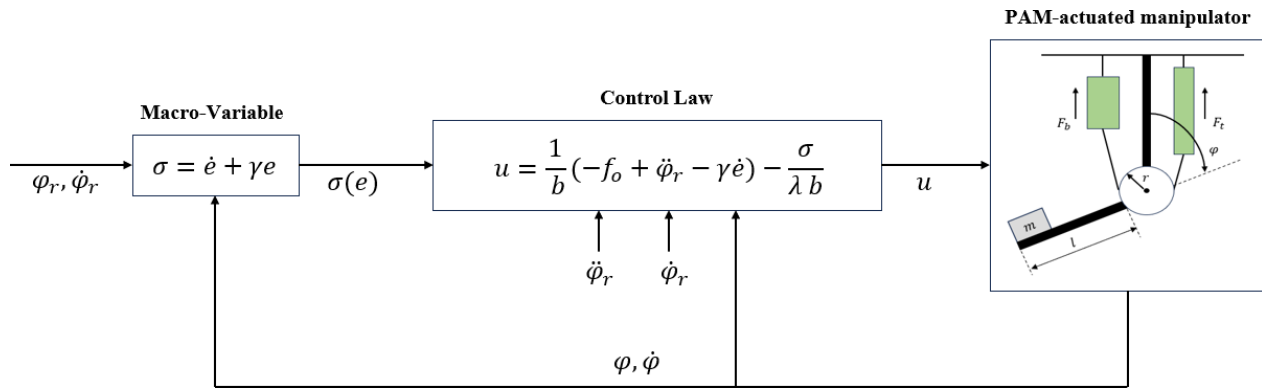
FIGURE 3. PAM-actuated manipulator controlled by SACT.

results in the form of more effectively dynamic performance of controlled systems. As a result, the Social Spider Optimisation (SSO) technique has been proposed as a method to discover the ideal values of these parameters in order to ensure excellent performance of the proposed controllers in terms of dynamic response. The design parameters for SMC are (c, k, β), while for SACT, they are (γ, λ).

Erik Cuevas et al. [22] established the SSO method, which models the cooperative behaviour of social spiders. SSO considers two search agents (spiders), one male and one female. Each individual is treated with a unique set of evolutionary operators based on its gender, which simulates various cooperative behaviours present in the colony. The flowchart of the SSO algorithm is shown in Figure 4. Like many metaheuristic algorithms, the performance of SSO depends on its parameter settings, such as population size, neighbourhood size, and movement parameters. These parameters often require fine-tuning to achieve good performance on different optimisation problems. In our design, the Integral of Time-Weighted Absolute Error (ITAE) was used to evaluate the cost of each individual during the search for choosing the best value with minimum cost for all controllers. The mathematical formula of ITAE is shown in Equation (41). The SSO algorithm has been run by setting several iterations equal to 32, and 60 for the number of spiders.

$$f = \text{ITAE} = \int_0^T t \cdot |e| \; dt. \tag{41}$$

4. COMPUTER SIMULATION

The physical parameters of the single link robotic arm actuated by PAMs are listed in Table 1 [5, 15]. A model of the robot incorporating the proposed controllers has been created using MATLAB/Simulink and the "Ode45" is used as the numerical solver. The results of the optimisation process based on the SSO are given in Table 2. Also, the behaviour of the cost function during the entire optimisation process with the design parameters for both the SACT and SMC controllers is shown in Figure 5.

The desired input signal applied for the controlled system is given by equation:

$$\begin{aligned} \varphi_r = \frac{\pi}{2} &+ 0.5 \left(\sin(2\pi f_1 t) \right. \\ &+ \left. \sin(2\pi f_2 t) + \sin(2\pi f_3 t) \right), \end{aligned} \tag{42}$$

where, $f_1 = 20 \, \text{mHz}$, $f_2 = 50 \, \text{mHz}$ and $f_3 = 90 \, \text{mHz}$.

The response of the robotic system with tracking behaviour for an angular position in terms of an uncertainty-free system is shown in Figure 6 and the angular velocity response of the same descriptive system is illustrated in Figure 7. Figures 8 and 9 show the behaviour of the control signals and the error signals resulting from the used controllers, respectively. The control system's performance based on SACT and SMC is reported in Table 3. The evaluation of the performance is based on root mean square error, steady-state errorm and settling time. From the previous results, we can see that the PAM system based on SACT was able to complete the trajectory tracking with high motion accuracy as compared to the one based on SMC.

After evaluating the results in terms of an uncertainty-free system, an uncertainty within 10 % of the nominal value was applied in the second case. Figures 10 and 11 show the tracking performance of both the angular position and velocity through the two controllers used sequentially. While Figures 12 and 13 show the behaviour of the control signal and error signal that have resulted from the applied controllers. Hence, from the provided results, it can clearly be seen that the SMC controller has failed to maintain the stability of the system as compared to the SACT controller.

5. CONCLUSION

In this work, a synergetic algorithm control theory and a sliding mode control method are developed for tracking PAM system control. These two control theories with their control laws were used to maintain the asymptotic stability of the system. The robustness and effectiveness of the proposed control schemes have been verified by several simulation studies. According to the simulation results, the SACT showed
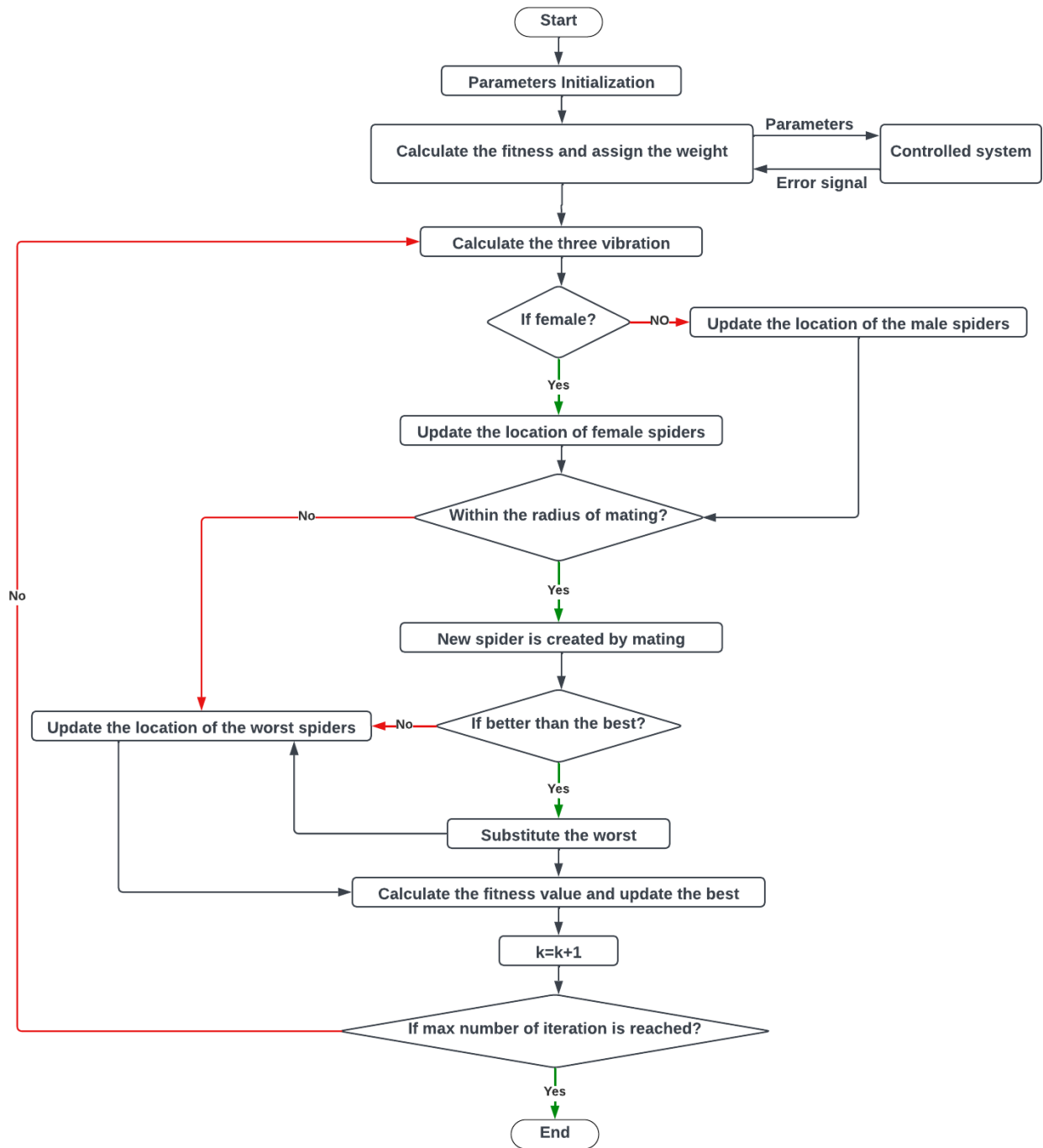
FIGURE 4. SSO flowchart.

Parameter	Value	Unit
m	20	kg
l	0.5	m
I	1.667	$\mathrm{kg\,m^{-2}}$
g	9.81	$\mathrm{m\,s^{-2}}$
r	0.05	m
P_{0b}	400	kPa
P_{0t}	400	kPa

TABLE 1. The parameters of single link robotic arm.

Controller	Optimal values	
	Coefficient	Value
SACT	γ	1.4558
	λ	0.0055
SMC	c	1.5278
	k	0.9997
	β	17.6440

TABLE 2. The proposed values of the design parameters for SACT and SMC by the SSO algorithm.

(A). SMC.

(B). SACT.
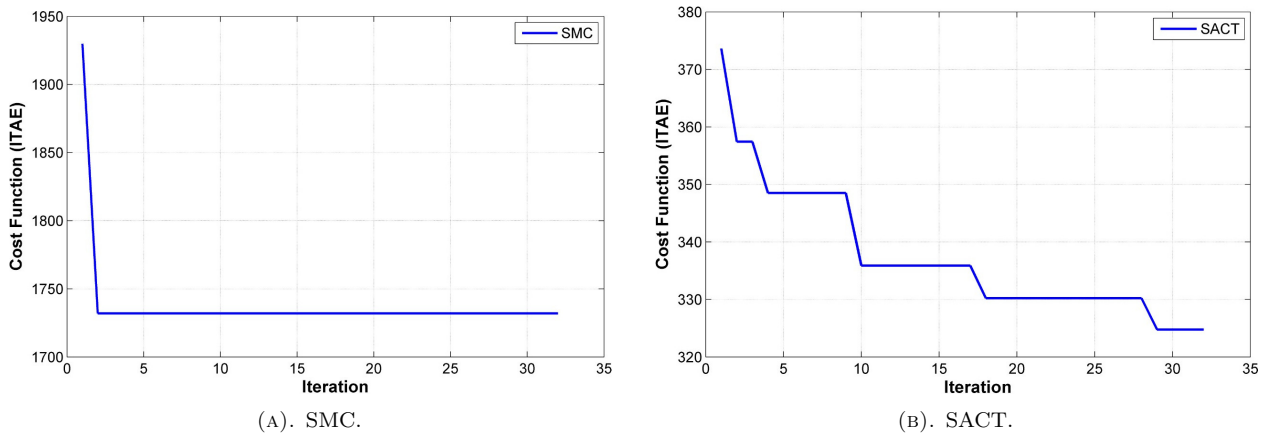
FIGURE 5. Evolution of the cost function versus the iterations.

Controller	RMSE	Settling time [sec]	Steady-state error [rad]	ITAE
SACT	0.0499	3.1	1.5×10^{-5}	324.8
SMC	0.1080	4.6	9.8×10^{-5}	1 732

TABLE 3. Evaluation of PAM-actuated manipulator controlled using SACT and SMC.
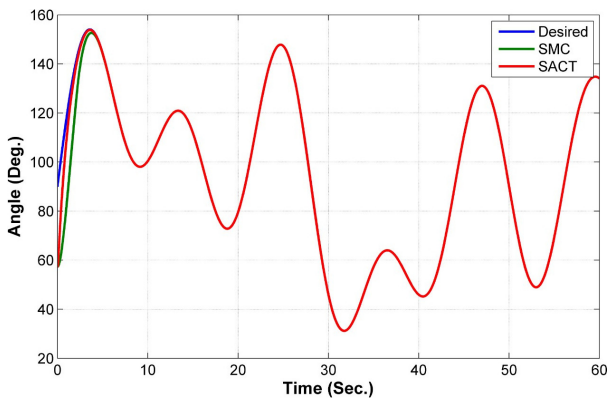
FIGURE 6. The behaviour of angular position without uncertainty.
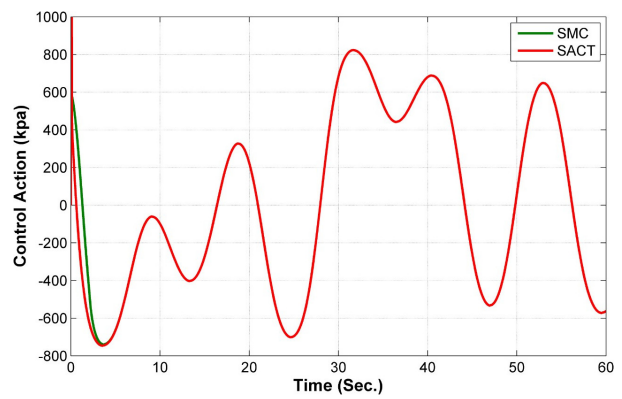
FIGURE 8. The behaviour of control action without uncertainty.
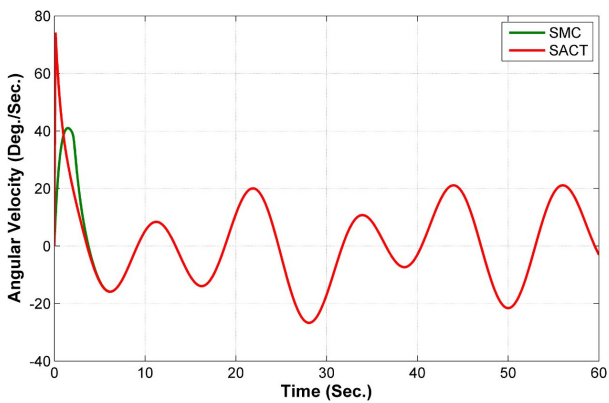
FIGURE 7. The behaviour of angular velocity without uncertainty.
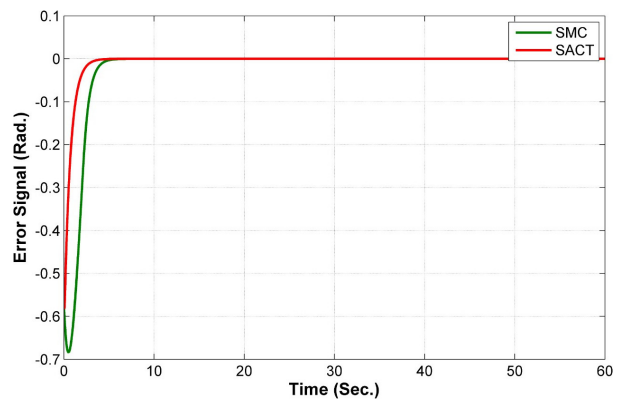
FIGURE 9. The behaviour of angle error signal without uncertainty.
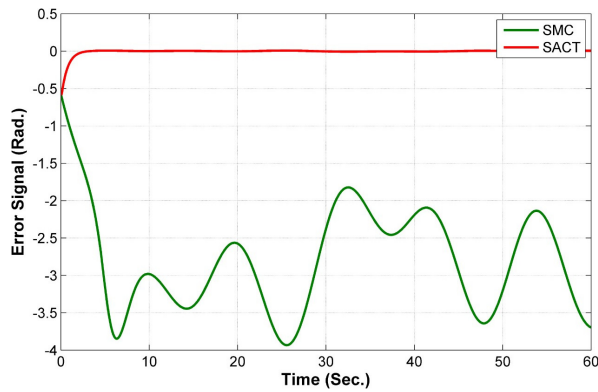
FIGURE 10. The behaviour of angle error signal with 10 % uncertainty in parameters.
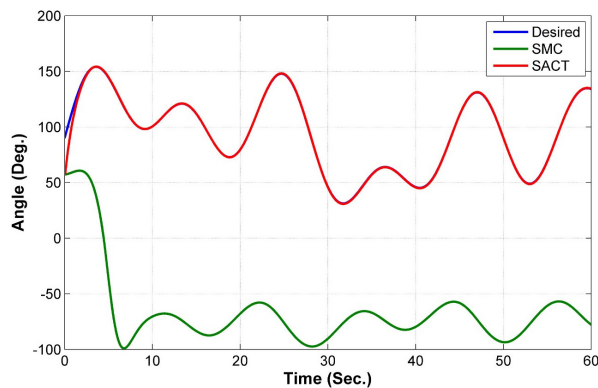
FIGURE 11. The behaviour of angular position with 10 % uncertainty in parameters.
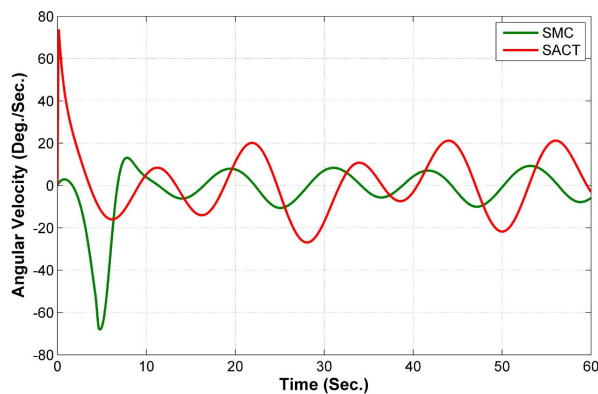
FIGURE 12. The behaviour of angular velocity with 10 % uncertainty in parameters.
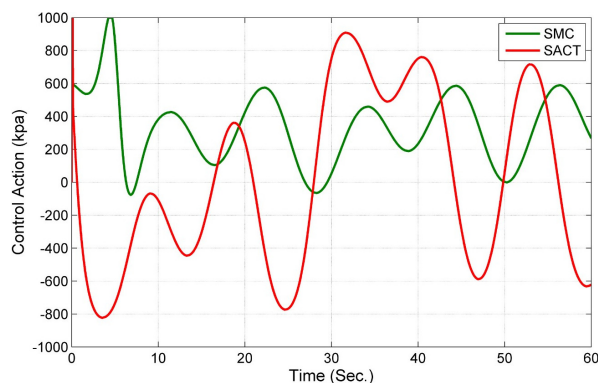
FIGURE 13. The behaviour of control action with 10 % uncertainty in parameters.

a better tracking performance and super robust characteristics against variations of the parameter's values than the SMC. The sample results obtained show that the SACT has a lower root mean square error (RMSE), 53.79 %, than the SMC. In addition, a further performance improvement was achieved with the two presented control schemes by using the SSO algorithm.

Future research endeavours of this study; one can suggest a two or three degree of freedom robot manipulator and use the same control techniques to show the robustness of SACT. Another suggestion is to use different optimisation techniques, such as the Whale Optimisation Algorithm (WOA) [23], Spotted Hyena Optimiser (SHO) [24], and Sparrow Search Optimisation [25] to make a comparison with those used in this study. One can propose other control strategies, such as Model Reference Adaptive Control (MRAC), observer-based control, robust control, backstepping control, Active Disturbance Reject Control (ADRC), and nonlinear PD control to further improve the proposed controller as future extension of this study [26–37].

REFERENCES

[1] R. M. Robinson, C. S. Kothera, R. M. Sanner, N. M. Wereley. Nonlinear control of robotic manipulators driven by pneumatic artificial muscles. *IEEE/ASME Transactions on Mechatronics* **21**(1):55–68, 2016. https://doi.org/10.1109/TMECH.2015.2483520

[2] H. Khajehsaeid, B. Esmaeili, R. Soleymani, A. Delkhosh. Adaptive back stepping fast terminal sliding mode control of robot manipulators actuated by pneumatic artificial muscles: continuum modelling, dynamic formulation and controller design. *Meccanica* **54**(8):1203–1217, 2019. https://doi.org/10.1007/s11012-019-01012-4

[3] M. Khaleel Ahmed, M. Majid Msallam. Enhancement performance of hydraulic actuators using PSO with FOPID controller. *Journal of Mechatronics and Artificial Intelligence in Engineering* **2**(1):19–29, 2021. https://doi.org/10.21595/jmai.2021.21872

[4] J. H. Lilly, L. Yang. Sliding mode tracking for pneumatic muscle actuators in opposing pair configuration. *IEEE Transactions on Control Systems Technology* **13**(4):550–558, 2005. https://doi.org/10.1109/TCST.2005.847333

[5] A. Al-Jodah, L. Khames. Second order sliding mode controller design for pneumatic artificial muscle. *Journal of Engineering* **24**(1):159–172, 2018. https://doi.org/10.31026/j.eng.2018.01.11

[6] W. Scaff, O. Horikawa, M. S. G. Tsuzuki. Pneumatic artificial muscle optimal control with simulated annealing. *IFAC-PapersOnLine* **51**(27):333–338, 2018. https://doi.org/10.1016/j.ifacol.2018.11.618

[7] S. Boudoua, M. Hamerlain, F. Hamerlain. Intelligent twisting sliding mode controller using neural network for pneumatic artificial muscles robot arm. In *International Workshop on Recent Advances in Sliding Modes (RASM)*, pp. 1–6. 2015. https://doi.org/10.1109/RASM.2015.7154592

[8] D. W. Repperger, C. A. Phillips, M. Krier. Controller design involving gain scheduling for a large scale pneumatic muscle actuator. In *Proceedings of the 1999 IEEE Conference on Control Applications*, vol. 1, pp. 285–290. 1999.
https://doi.org/10.1109/cca.1999.806643

[9] A. Enzevaee, M. Mailah, S. Kazi. Control of a single link robot arm actuated by pneumatic artificial muscles employing active force control and fuzzy logic via hardware-in-the-loop-simulation. *Jurnal Mekanikal* **36**(2):66–85, 2013.

[10] M. Farag, N. Z. Azlan. Adaptive backstepping position control of pneumatic anthropomorphic robotic hand. *Procedia Computer Science* **76**:161–167, 2015.
https://doi.org/10.1016/j.procs.2015.12.334

[11] S. M. Mahdi, N. Q. Yousif, A. A. Oglah, et al. Adaptive synergetic motion control for wearable knee-assistive system: A rehabilitation of disabled patients. *Actuators* **11**(7):176, 2022.
https://doi.org/10.3390/act11070176

[12] E. Nechadi, M. N. Harmas, N. Essounbouli, A. Hamzaoui. Optimal synergetic control based Bat algorithm for DC-DC boost converter. *IFAC-PapersOnLine* **49**(12):698–703, 2016.
https://doi.org/10.1016/j.ifacol.2016.07.792

[13] A. Q. Al-Dujaili, A. J. Humaidi, Z. T. Allawi, M. E. Sadiq. Earthquake hazard mitigation for uncertain building systems based on adaptive synergetic control. *Applied system innovation* **6**(2):34, 2023.
https://doi.org/10.3390/asi6020034

[14] H. Al-Khazraji, K. Albadri, R. Almajeez, A. J. Humaidi. Synergetic control-based sea lion optimization approach for position tracking control of ball and beam system. *International Journal of Robotics and Control Systems* **4**(4):1547–1560, 2024.
https://doi.org/10.31763/ijrcs.v4i4.1551

[15] D. W. Repperger, K. R. Johnson, C. A. Phillips. VSC position tracking system involving a large scale pneumatic muscle actuator. In *Proceedings of the 37th IEEE Conference on Decision and Control*, vol. 4, pp. 4302–4307. 1998.
https://doi.org/10.1109/cdc.1998.761982

[16] İ. Haskara, C. Hatipoğlu, Ü. Özgüner. *Variable Structure Systems: Towards the 21st Century*, chap. Sliding Mode Compensation, Estimation and Optimization Methods in Automotive Control, pp. 155–174. 2007.
https://doi.org/10.1007/3-540-45666-x_7

[17] C.-J. Lin, T.-Y. Sie, W.-L. Chu, et al. Tracking control of pneumatic artificial muscle-activated robot arm based on sliding-mode control. *Actuators* **10**(3):66, 2021. https://doi.org/10.3390/act10030066

[18] S. A. Al-Samarraie, S. D. Salman. Backstepping nonlinear control for blood glucose based on sliding mode meal observer. *Al-Nahrain Journal for Engineering Sciences* **21**(3):436–444, 2018.
https://doi.org/10.29194/njes.21030436

[19] A. Kolesnikov, R. Dougal, G. E. Veselov, et al. Synergetic control for electromechanical systems. In *15th International Symposium on Mathematical Theory of Networks and Systems*, pp. 1–8. 2002.

[20] M. Zhao, T. Wang. A sliding mode and synergetic control approaches applied to permanent magnet synchronous motor. *Journal of Physics: Conference Series* **1087**(4):042012, 2018.
https://doi.org/10.1088/1742-6596/1087/4/042012

[21] A. F. Mutlak, A. J. Humaidi. Adaptive synergetic control for electronic throttle valve system. *International Review of Applied Sciences and Engineering* **15**(2):211–220, 2024.
https://doi.org/10.1556/1848.2023.00706

[22] E. Cuevas, M. Cienfuegos, D. Zaldívar, M. Pérez-Cisneros. A swarm optimization algorithm inspired in the behavior of the social-spider. *Expert Systems with Applications* **40**(16):6374–6384, 2013.
https://doi.org/10.1016/j.eswa.2013.05.041

[23] N. Rana, M. S. A. Latiff, S. M. Abdulhamid, H. Chiroma. Whale optimization algorithm: A systematic review of contemporary applications, modifications and developments. *Neural Computing and Applications* **32**(20):16245–16277, 2020.
https://doi.org/10.1007/s00521-020-04849-z

[24] G. Dhiman, A. Kaur. Optimizing the design of airfoil and optical buffer problems using spotted hyena optimizer. *Designs* **2**(3):28, 2018.
https://doi.org/10.3390/designs2030028

[25] H. Al-Khazraji, K. Al-Badri, R. Al-Majeez, A. J. Humaidi. Synergetic control design based sparrow search optimization for tracking control of driven-pendulum system. *Journal of Robotics and Control (JRC)* **5**(5):1549–1556, 2024.
https://doi.org/10.18196/jrc.v5i5.22893

[26] A. J. Humaidi, A. H. Hameed. Robustness enhancement of MRAC using modification techniques for speed control of three phase induction motor. *Journal of Electrical Systems* **13**(4):723–741, 2017.

[27] A. J. Humaidi, E. N. Talaat, M. R. Hameed, A. H. Hameed. Design of adaptive observer-based backstepping control of cart-pole pendulum system. In *Proceedings of 2019 3rd IEEE International Conference on Electrical, Computer and Communication Technologies (ICECCT)*, pp. 1–5. 2019.
https://doi.org/10.1109/ICECCT.2019.8869179

[28] A. S. Aljuboury, A. H. Hameed, A. R. Ajel, et al. Robust adaptive control of knee exoskeleton-assistant system based on nonlinear disturbance observer. *Actuators* **11**(3):78, 2022.
https://doi.org/10.3390/act11030078

[29] A. J. Humaidi, S. K. Kadhim, A. S. Gataa. Optimal adaptive magnetic suspension control of rotary impeller for artificial heart pump. *Cybernetics and Systems* **53**(1):141–167, 2022.
https://doi.org/10.1080/01969722.2021.2008686

[30] A. A. Oglah, M. M. Msallam. Real-time implementation of Fuzzy Logic Controller based on chicken swarm optimization for the ball and plate system. *International Review of Applied Sciences and Engineering* **13**(3):263–271, 2021.
https://doi.org/10.1556/1848.2021.00360

[31] A. J. Humaidi, S. K. Kadhim, A. S. Gataa. Development of a novel optimal backstepping control algorithm of magnetic impeller-bearing system for artificial heart ventricle pump. *Cybernetics and Systems* **51**(4):521–541, 2020. https://doi.org/10.1080/01969722.2020.1758467

[32] A. J. Humaidi, M. R. Hameed. Design and performance investigation of block-backstepping algorithms for ball and arc system. In *2017 IEEE International Conference on Power, Control, Signals and Instrumentation Engineering (ICPCSI)*, pp. 325–332. IEEE, 2017. https://doi.org/10.1109/ICPCSI.2017.8392309

[33] A. J. Humaidi, M. R. Hameed, A. H. Hameed. Design of block-backstepping controller to ball and arc system based on zero dynamic theory. *Journal of Engineering Science and Technology* **13**(7):2084–2105, 2018.

[34] A. J. Humaidi, A. I. Abdulkareem. Design of augmented nonlinear PD controller of Delta/Par4-like Robot. *Journal of Control Science and Engineering* **2019**(1):7689673, 2019. https://doi.org/10.1155/2019/7689673

[35] W. R. Abdul-Adheem, A. T. Azar, I. K. Ibraheem, A. J. Humaidi. Novel active disturbance rejection control based on nested linear extended state observers. *Applied Sciences* **10**(12):4069, 2020. https://doi.org/10.3390/app10124069

[36] A. S. M. Al-Obaidi, A. Al-Qassar, A. R. Nasser, et al. Embedded design and implementation of mobile robot for surveillance applications. *Indonesian Journal of Science and Technology* **6**(2):427–440, 2021. https://doi.org/10.17509/ijost.v6i2.36275

[37] R. A. Kadhim, M. Q. Kadhim, H. Al-Khazraji, A. J. Humaidi. Bee algorithm based control design for two-links robot arm systems. *IIUM Engineering Journal* **25**(2):367–380, 2024. https://doi.org/10.31436/iiumej.v25i2.3188